Vectorially Oriented Membrane Protein Monolayers: Profile Structures via X-Ray Interferometry/Holography

Janine A. Chupa, John P. McCauley, Jr., Robert M. Strongin, Amos B. Smith III, J. Kent Blasie, Lawrence J. Peticolas,* and John C. Bean*

Department of Chemistry, University of Pennsylvania, Philadelphia, Pennsylvania 19104, and *AT&T Bell Laboratories, Murray Hill, New Jersey 07974 USA

ABSTRACT X-ray interferometry/holography was applied to meridional x-ray diffraction data to determine uniquely the profile structures of a single monolayer of an integral membrane protein and a peripheral membrane protein, each tethered to the surface of a solid inorganic substrate. Bifunctional, organic self-assembled monolayers (SAMs) were utilized to tether the proteins to the surface of Ge/Si multilayer substrates, fabricated by molecular beam epitaxy, to facilitate the interferometric/holographic x-ray structure determination. The peripheral membrane protein yeast cytochrome *c* was covalently tethered to the surface of a sulfhydryl-terminated 11-siloxyundecanethiol SAM via a disulfide linkage with residue 102. The detergent-solubilized, photosynthetic reaction center integral membrane protein was electrostatically tethered to the surface of an analogous amine-terminated SAM. Optical absorption measurements performed on these two tethered protein monolayer systems were consistent with the x-ray diffraction results indicating the reversible formation of densely packed single monolayers of each fully functional membrane protein on the surface of the respective SAM. The importance of utilizing the organic self-assembled monolayers (as opposed to Langmuir-Blodgett) lies in their ability to tether specifically both soluble peripheral membrane proteins and detergent-solubilized integral membrane proteins. The vectorial orientations of the cytochrome *c* and the reaction center molecules were readily distinguishable in the profile structure of each monolayer at a spatial resolution of 7 Å.

INTRODUCTION

The study of reconstituted membrane systems containing selected molecular components involved in biological electron transfer has been successful in providing structural information on their supramolecular organization (Pachence et al., 1979, 1981, 1983; Blasie et al., 1983). Correlations of such structural information with functional characteristics in these systems are fundamental to the understanding of energy conversion processes (Gunner et al., 1986; Alegria and Dutton, 1991). For example, previous structural studies on thick, oriented multilayers of reconstituted membranes containing phosphatidylcholine and photosynthetic reaction center protein from *Rhodopseudomonas sphaeroides* established the profile structure of the integral membrane protein and its position relative to the lipid bilayer (Pachence et al., 1979, 1981). Further structural studies of the peripheral membrane protein cytochrome *c* bound to the reaction center protein in such reconstituted membranes yielded the position of the cytochrome *c* molecule relative to the reaction center molecule in the membrane profile (Pachence et al., 1983). Resonance x-ray diffraction from these reconstituted cytochrome *c*/reaction center/phospholipid membrane multilayers then provided the distance across the membrane profile separating the cytochrome heme iron atom electron donor and the iron atom coupled to the primary quinone electron acceptor in the reaction center protein (Blasie et al., 1983). Such structural studies, in general, cannot be extended to other integral membrane protein systems because of the lack of a unique vectorial orientation for the membrane protein molecules incorporated into the vesicle lipid bilayer (see, for example, Stamatoff et al., 1982; Blasie et al., 1982), as happened to be the case for the reaction center protein work. This limitation resulted in the subsequent work to develop a more general approach for the reconstitution of membrane molecular components to form two-dimensionally dense monolayers with macroscopic in-plane dimensions in which the protein molecules possessed a unique or "unidirectional" vectorial orientation (the three-dimensional structure of a protein molecule at atomic resolution is, in general, asymmetric; hence, the orientation of the protein molecule in 3-D space can be represented by a single vector referenced to some convenient aspect of the protein's physical-chemical structure within the internal coordinate frame of the molecule. For membrane proteins, "vectorial orientation" refers to the orientation of that vector representing the internal coordinate frame of the protein molecule *relative* to the coordinate frame of the host membrane, for example, either the plane of the membrane or the normal to that plane).

Structural studies on the protein monolayer system consisting of an ultrathin fatty acid multilayer film on a solid substrate, formed using the Langmuir-Blodgett (LB) technique, possessing a surface monolayer of electrostatically tethered horse heart cytochrome *c* firmly established the presence and position of the protein monolayer with respect to the profile structure of the lipid multilayer film, using both nonresonance and resonance x-ray diffraction (Pachence and Blasie, 1987; Pachence et al., 1989; Pachence and Blasie, 1991). Optical linear dichroism was then used to determine the orientation of the heme group and, hence, the vectorial

Received for publication 16 November 1993 and in final form 28 April 1994.

Address reprint requests to Janine A. Chupa, Department of Chemistry, University of Pennsylvania, 231 South 34th Street, Philadelphia, PA 19104-6323. Tel.: 215-898-2097; Fax: 215-898-6242.

0006-3495/94/07/336/13 $2.00

orientation of the protein molecule, for both electrostatically tethered horse heart and covalently tethered yeast cytochrome *c* on the surface of ultrathin lipid multilayer films (Pachence et al., 1990). The analysis of the x-ray diffraction data providing the profile structures of the ultrathin lipid multilayers having either an electrostatically or covalently tethered surface layer of cytochrome *c* employed a nonunique box refinement method (Pachence and Blasie, 1991). Although these LB films were capable of specifically binding the soluble, peripheral membrane proteins such as cytochrome *c*, this method could not be extended to integral membrane proteins that are solubilized using detergents, such as the photosynthetic reaction center, because they would be expected to dissolve the lipid layers of the LB films.

Therefore, to accommodate integral membrane proteins in such vectorially oriented protein monolayer systems having macroscopic in-plane dimensions, recent structural studies were performed on single monolayers of yeast cytochrome *c*, and its bimolecular electrostatic complex with the photosynthetic reaction center, covalently tethered to self-assembled monolayers (SAMs) of 11-siloxyundecanethiol on inorganic substrates (Amador et al., 1993). These tethered SAM/protein systems were formed on the surfaces of sputtered Ge/Si multilayer substrates to determine their profile structures from the meridional x-ray diffraction using x-ray interferometry (Lesslauer and Blasie, 1971; Xu et al., 1991), where the known multilayer substrate structure acts as the reference structure employed to determine the unknown structure of the adjacent SAM/protein overlayer. The Ge and Si layer thicknesses in the sputtered multilayer substrates were both limited to >20 Å, which resulted in the characterization of the profile structures from the meridional x-ray diffraction to an effective spatial resolution of >20 Å. This relatively low resolution proved, unfortunately, to be insufficient to establish firmly the vectorial orientation of the reaction center within the tethered, bimolecular cytochrome *c*/reaction center complex.

This study extends the previous work on sputtered substrates by using Ge/Si multilayer substrates fabricated by molecular beam epitaxy (MBE) in which the Ge layer thicknesses are significantly thinner than in the sputtered substrates, being limited in principle to the thickness of a single Ge atomic monolayer of ~3.5 Å. As a result, data collection in this work, employing only two atomic monolayers of Ge in the Ge layers, was extended to an improved spatial resolution of ~7 Å. Furthermore, the thinness of the Ge layers permitted the utilization of x-ray holography to prove the correctness of the monolayer profile structures derived by x-ray interferometry. We chose to study two model systems, yeast cytochrome *c* covalently tethered to 11-siloxyundecanethiol SAMs and photosynthetic reaction centers electrostatically tethered to 11-siloxyundecaneamine SAMs, on MBE substrates, because both the cytochrome *c* and photosynthetic reaction center protein structures are known to atomic resolution, which was expected thereby to facilitate the assessment of the utility of the self-assembly process to produce vectorially oriented protein monolayers. In addition, these proteins participate in biologically important electron transfer reactions facilitating the study of structure-function correlations. Schematics of these model systems are shown in Fig. 1, *a* and *b*, where the proteins are represented by their crystal structures. Yeast (*Saccharomyces cerevisiae*) cytochrome *c*, which differs from other species in that it possesses a surface cysteine residue located near the carboxy-terminus at sequence position 102, previously has been found to form covalent disulfide bonds with extrinsic thiol groups (Bill et al., 1980), including those of the 11-siloxyundecanethiol SAM (Amador et al., 1993). In this study, we show that the reaction center species used (*Rhodopseudomonas sphaeroides*), containing no endogenous *c*-type cytochrome heme, can be bound electrostatically directly to an 11-siloxyundecaneamine SAM, where the amine surface endgroups presumably mimic the lysine and arginine residues of cytochrome *c*. Comparisons are made between the results of these structural studies and the earlier results on protein monolayer systems. In particular, the utilization of the self-assembly method is discussed as a vehicle to investigate the structural organization of monolayers of other vectorially oriented integral membrane proteins, such as cytochrome oxidase and cytochrome b/c_1.

MATERIALS AND METHODS

The Ge/Si multilayer substrates, used in the x-ray diffraction experiments, were prepared by MBE at AT&T Bell Laboratories (Bean and Sadowski, 1982). These substrates were grown on 4 inch N-type Si(100) wafers (Monsanto, St. Louis, MO) with a resistivity of 0.005 ohm cm. A smoothed Si surface was initially produced by depositing a (Si_{30}) layer, i.e., 30 atomic monolayers of Si, onto the Si(100) wafer. A two unit cell superlattice structure of the form 2(Ge_2Si_{30}) was then fabricated by subsequent depositions of Ge and Si atomic monolayers. Details of the MBE procedures are referenced (Bean et al., 1984). The superlattice unit cell, consisting of the Ge/Si "bilayer" (Ge_2Si_{30}), has a profile thickness of ~36 Å, which was selected to coincide roughly with that of the various organic/bio-organic overlayers to be tethered to the substrate's surface (Xu et al., 1993; Murphy et al., 1993), thereby generating strong meridional x-ray diffraction from the reference Ge/Si multilayer structure over the corresponding region of reciprocal space perpendicular to the substrate plane, i.e., along the q_z axis, where x-ray scattering from the unknown overlayer was also expected to be strong. By using only two superlattice unit cells in the inorganic reference structure, continuous meridional x-ray diffraction is generated over a wide range of q_z. This guarantees the maximum amount of interference with the scattering from the unknown organic/bio-organic overlayer. Furthermore, the more electron-dense Ge layer was chosen to be very thin, resulting in considerably more intense x-ray diffraction out to larger q_z for the MBE reference structure substrates, in contrast to those used previously produced by magnetron sputtering (Amador et al., 1993; Xu et al., 1991). The wafers were cut with a diamond pencil to obtain 2 cm × 1 cm × 30 mil substrates.

Two organic compounds were synthesized to produce the SAMs possessing appropriate functional endgroups. The thiol-terminated SAMs were prepared using 11-trichlorosilylundecyl thioacetate, synthesized according to Wasserman et al. (1989), with all compounds purchased from Aldrich (Milwaukee, WI). 11-*N*-(*tert*-butoxycarbonyl)-aminoundecyltriethoxysilane was the precursor for the amine-terminated SAM. To obtain this compound (all compounds purchased from Aldrich, Milwaukee, WI), 10-undecylenylazide was first synthesized via treatment of 10-undecylenylbromide with sodium azide in dimethylformamide for 24 h at room temperature and was subsequently converted to the primary amine via reduction with triphenylphosphine and water in tetrahydrofuran solvent at room temperature over 4 h. The amine was not isolated, and the crude

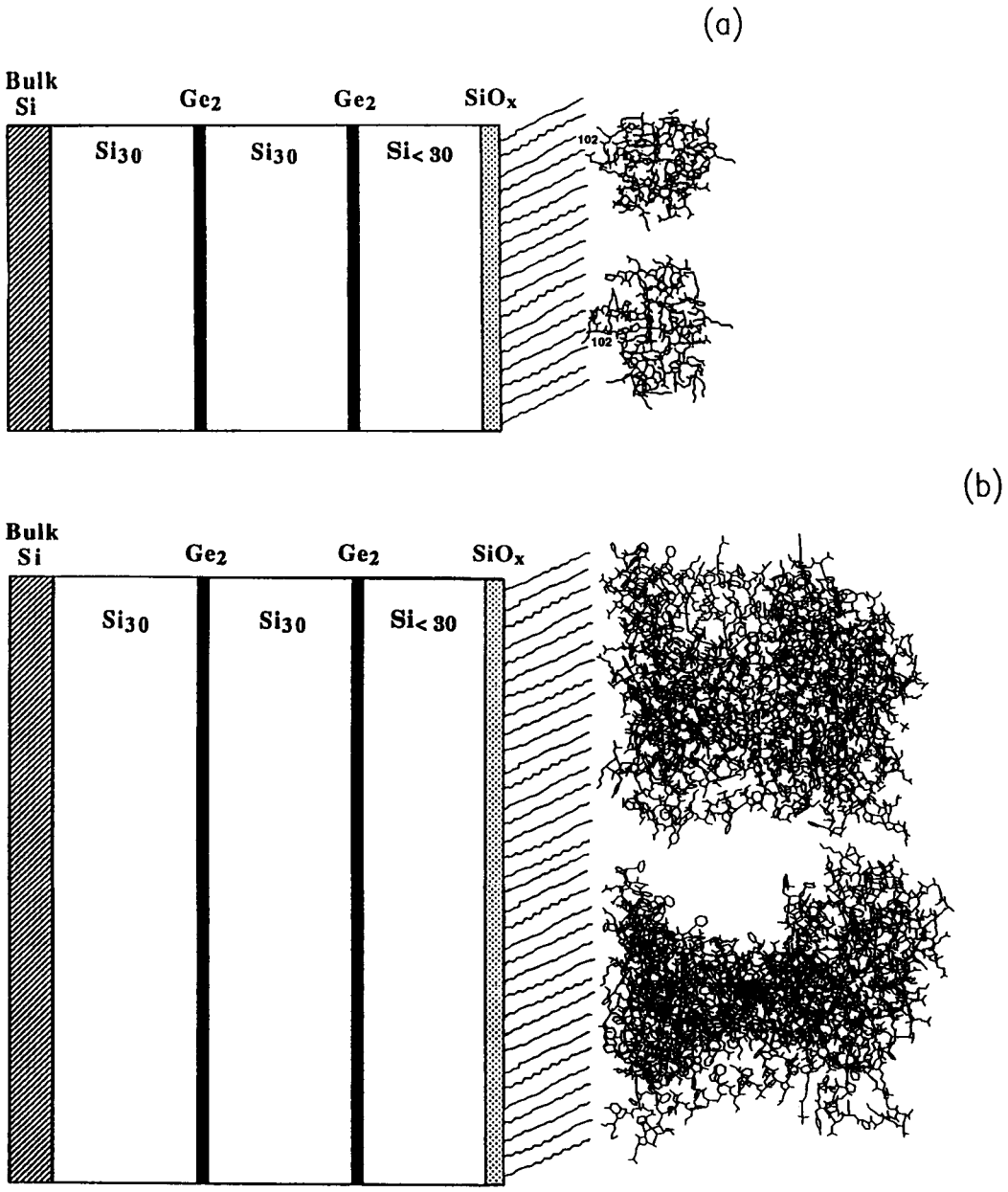

FIGURE 1 Schematics of the SAM/tethered protein systems on the Ge/Si multilayer substrates. The proteins are each shown as representations of their x-ray crystal structures for two orientations about the axis of rotation, which is perpendicular to the monolayer plane. Although the chain tilt angle has not been directly measured for these particular SAM systems, we feel that it is more general to represent the chains tilted arbitrarily from the normal to the substrate plane, as has been demonstrated for methyl-terminated chains (Xu et al., 1993). Only a portion of the $2(Ge_2Si_{30})$ substrate, fabricated by molecular beam epitaxy, is shown. (*a*) A yeast cytochrome *c* molecule covalently tethered to an 11-siloxyundecanethiol SAM on a MBE substrate. The Cys-102 residue, responsible for the covalent tethering of the protein, is labeled. (*b*) A photosynthetic reaction center molecule electrostatically bound to an 11-siloxyundecaneamine SAM on a MBE substrate. The slight height difference in the two orientations of the reaction center results from an artifact in the gray-scale plotting program, which shades the residues relative to their distance from the surface of the molecule.

mixture was further treated with di-*tert*-butyl dicarbonate in methylene chloride at room temperature to yield 11-*N*-(*tert*-butoxycarbonyl)-aminoundecene. Hydrosilylation (Lukevics et al., 1977; Wasserman et al., 1989) via reaction with triethoxysilane and hydrogen hexachloroplatinate (IV) hydrate for 48 h at 93°C yielded, upon distillation, the precursor 11-*N*-(*tert*-butoxycarbonyl)-aminoundecyltriethoxysilane. Satisfactory IR, 500-MHz ^{1}H NMR, and 62.5-MHz ^{13}C NMR spectra were obtained for this compound. Another amine-terminated SAM has been referenced (Balachander and Sukenik, 1988). The SAMs were formed on the surface of glass substrates ($11 \times 25 \times 1$ mm^3) for the optical absorption spectroscopy and the Ge/Si multilayer substrates by following the general alkylation procedure by Sagiv (1980). Modifications have been described previously (Xu et al., 1993). The SAMs were activated by removing the protecting acetate and *tert*-butoxycarbonyl groups for the thiol- and amine-terminated SAMs, respectively, achieved via acid hydrolysis (soaking substrates held in a wafer basket contained in a crystallizing dish in concentrated HCl for 1.5 h). After rinsing in >3 l of ultrapure water, the SAM-coated substrates were immediately immersed in vials of the corresponding protein solution prepared in 1 mM TRIS-HCl buffer at pH 8. The thiol-terminated SAMs were incubated for ~24 h in 15 μM yeast cytochrome *c* from *Saccharomyces cerevisiae*

(Sigma Chemical Co., St. Louis, MO). The amine-terminated SAMs were incubated for ~72 h in solutions of 5–10 μM photosynthetic reaction centers from *Rhodopseudomonas sphaeroides* in 1 mM TRIS buffer at pH 8 with 0.1% lauryldimethylamine oxide (LDAO) detergent. The reaction centers were purified and resuspended in LDAO as reported previously (Clayton and Wang, 1971). Each sample was removed from its incubating protein solution and rinsed extensively (at least 6 times) in 1 mM TRIS pH 8 buffer to remove nonspecifically bound protein.

Optical absorption spectra were recorded for the SAM/protein specimens prepared on the glass substrates using a double-beam spectrophotometer (Hitachi Model U2000, San Jose, CA). These specimens and analogous reference specimens lacking only the protein, i.e., deprotected SAMs, were placed in quartz cuvettes (1 cm path length) in solutions of 1 mM TRIS pH 8 buffer and 1 mM sodium ascorbate, to reduce the cytochrome *c* or reaction centers.

Meridional x-ray diffraction data, as a function of $q_z = (2\sin\theta)/\lambda$ corresponding to elastic photon momentum transfer parallel to the *z* axis perpendicular to the substrate plane, were collected from the SAM/protein specimens prepared on the Ge/Si multilayer substrates, having already collected analogous data from the bare substrates. This meridional x-ray diffraction arises from the projection of the three-dimensional electron density distribution of the multilayer specimen along radial vectors perpendicular to the *z* axis onto the *z* axis; this projection is defined as the electron density profile, $\rho(z)$, for the sample. The incident x-ray beam defines an angle omega (ω) with the substrate (xy) plane. Meridional x-ray diffraction is observed for ω equal to θ, where 2θ is the angle between the incident and scattered beams.

The specimens were positioned on the ω axis of a Huber 4-circle diffractometer, which was oscillated over an appropriate range of ω values ($0.3° < \omega < 6.5°$) to generate meridional diffraction over $0.011\ \text{Å}^{-1} < q_z < 0.125\ \text{Å}^{-1}$, allowing for data collection using a two-dimensional, position-sensitive proportional counter (Siemens Instruments, Madison, WI) interfaced to a GPXII MicroVAX computer (Digital Equipment Corp., Marlboro, MA). Such meridional diffraction patterns were collected in sequential ~1 h time frames over a ~17-h period and stored as two-dimensional data files. Integration of these files perpendicular to the q_z axis over a width inclusive of the meridional diffraction produced a one-dimensional data file, i.e., total number of x-ray counts versus detector channel number along the q_z axis. No evolution of the meridional x-ray diffraction from any of the specimens was evident from subsequent examination of these one-dimensional data files collected over the ~17 h time period, as would be expected for radiation damage or other instabilities in the specimen.

Throughout data collection, the bare Ge/Si multilayer substrates and the protected SAM specimens were housed in an aluminum chamber with mylar windows in a dry helium atmosphere, maintained at room temperature (20.0 ± 0.5°C). The deprotected SAM and tethered protein monolayer specimens, housed in a chamber with aluminum foil windows, were maintained at 4.0 ± 0.5°C and a constant relative humidity (98 ± 1%) via a humidity controller during the experiment. The humidity controller, which was designed after the specifications published in the literature (Gruner, 1988) and fabricated by Dr. Francisco Asturias in our laboratory, consisted of an optical condensation dewpoint hygrometer (General Eastern Model 111H, Watertown, MA) to measure the relative humidity for a mixture of wet and dry helium gas controlled via a process controller (Omega Engineering Model 2101, Stamford, CT), with feedback from a monitor (General Eastern Model Hygro-M2) for the hygrometer. The humidity controller continuously circulated a small volume of the moist helium through the specimen chamber. An Elliott GX-13 rotating anode generator (Enraf-Nonius, Bohemia, NY) at a target loading of 27 kW/mm^2 was used to produce the Cu emission spectrum. The CuKα_1 line (λ = 1.541 Å) was selected using a 37 mm × 20 mm cylindrically bent Ge(111) monochromator crystal (Innovative Technology, Inc., South Hamilton, MA), resulting in a line-focused x-ray beam parallel to the ω axis. The specimen-to-detector distance was 350 mm, and the beam height at the specimen was 6 mm with incident and scattered beam paths in helium. The focused x-ray beam width at the detector and the spatial resolution of the two-dimensional detector system resulted in a Δq_z resolution of ~0.0009 Å^{-1}.

Meridional x-ray diffraction was also obtained for several of these specimens utilizing the Biostructures Participating Research Team beamline X-9A at the National Synchrotron Light Source (NSLS), Brookhaven National Laboratory (Upton, NY). The much more intense x-ray source allowed for better counting statistics at higher values of q_z as well as shorter data collection times. The synchrotron operated at an electron energy of 2.5 GeV, and the ring current decayed from 200 to 90 mA during a fill. A constant-exit-height, double Si(111) crystal monochromator was used to select the energy (8.041 keV) of the x-ray radiation, having a FWHM of 2.5 eV. A linearly collimated beam was obtained using a cylindrically bent horizontal mirror (Ni-coated Al) 1340 cm downstream from the bending-magnet source. The scattering geometry and other instrumental conditions were the same as those for the rotating anode x-ray source. An automated Al foil changer was used to attenuate the incident beam intensity to protect the total-count-rate limited detector. Multilayer specimens were oscillated over the full angular range $0.3° < \omega < 6.5°$ and over a more limited range $1.8° < \omega < 6.5°$ for better counting statistics data collection at higher values of q_z. Additional details of the diffraction conditions have been described previously (Fischetti et al., 1988).

RESULTS

The interaction between yeast cytochrome *c* and a thiol-terminated SAM was previously determined to be covalent (Pachence and Blasie, 1991; Amador et al., 1993). Fig. 2 *a* shows a typical optical absorption spectrum from reduced cytochrome *c* covalently bound to the surface of a thiol-terminated SAM. The absorbance in the α band at 550 nm of 0.002 OD was used to determine the concentration of the

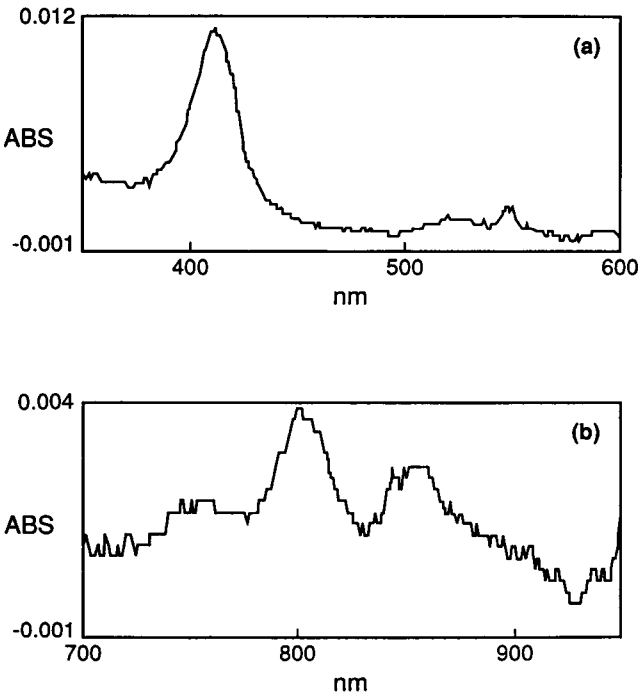

FIGURE 2 (*a*) Optical absorption spectrum for yeast cytochrome *c* covalently tethered to the surface of an 11-siloxyundecanethiol SAM on glass. The cytochrome *c* concentrations for the tethered monolayers were determined using the heme α band absorption peak signature for cytochrome *c* at 550 nm. (*b*) Near-IR absorption spectrum for photosynthetic reaction centers electrostatically tethered to the surface of an 11-siloxyundecaneamine SAM on glass. The reaction center concentrations for the tethered monolayers were determined using the chlorophyll 800 nm absorption peak.

cytochrome *c* on the SAM's surface using a molar extinction coefficient of $\epsilon_{550} = 29{,}500\ M^{-1}\ cm^{-1}$. This absorbance was determined previously to be consistent with a close-packed monolayer of cytochrome *c* (Pachence and Blasie, 1987; Steinemann and Lauger, 1971). The amine endgroups were chosen to resemble the lysine and arginine residues of cytochrome *c* for the electrostatic binding the reaction center protein directly to the surface of the SAM. A typical near-IR absorption spectrum for reaction center protein electrostatically bound to the surface of an amine-terminated SAM is shown in Fig. 2 *b*. The characteristic exciton band arising from the chlorophyll special pair at 865 nm indicates that the reaction center protein remains intact upon binding to the SAM surface. The absorbance of the 800-nm peak of 0.003 OD together with a molar extinction coefficient of $\epsilon_{800} = 2 \times 10^5\ M^{-1}\ cm^{-1}$ is consistent with a close-packed protein monolayer having 4.5×10^{12} RC molecules/cm^2. The reproducibility of the absorbance values for both the cytochrome *c* and reaction center samples was extremely high, with measurements made on greater than five batches of each SAM/protein type.

Figs. 3 *a* and 4 *a* show the meridional x-ray scattering data as $\ln[I(q_z)]$ for two bare Ge/Si multilayer substrates. Subsequently, a thiol-terminated SAM followed by a covalently bound surface layer of yeast cytochrome *c* protein were formed on the surface of one substrate, whereas an amine-terminated SAM followed by an electrostatically bound surface layer of photosynthetic reaction center protein were formed on the surface of the other substrate, which resulted in the meridional x-ray scattering data shown in Figs. 3 *b* and 4 *b*, respectively. The data at higher q_z have been expanded on a 10-fold scale. Because we were primarily interested in the kinematical diffraction within these data, the ω-oscillations were not extended down to the critical angle for the specular scattering from each specimen's surface, stopping instead at the equivalent reciprocal space $(q_z)_{min} \approx 0.010\ Å^{-1}$. For the specimens studied, meridional x-ray scattering above background scattering levels was observed generally out to $(q_z)_{max} \sim 0.125\ Å^{-1}$, with a good signal-to-noise ratio.

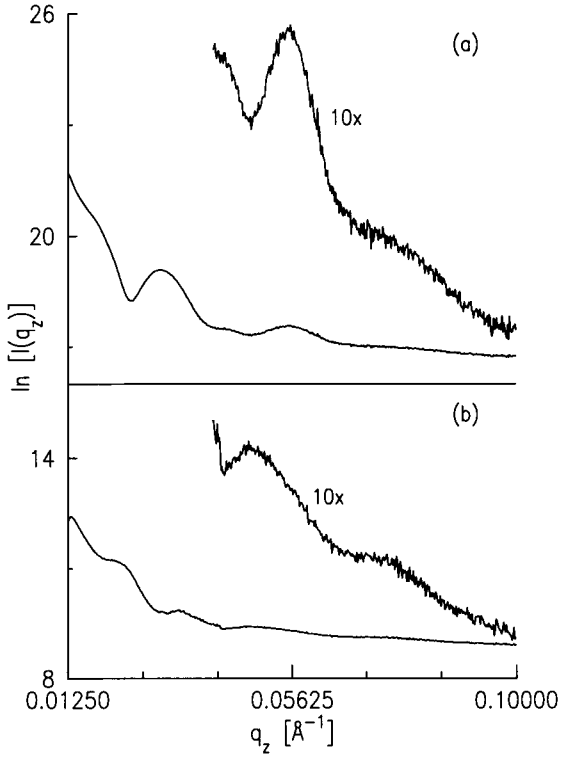

FIGURE 3 Meridional x-ray scattering data, $\ln[I(q_z)]$, for (*a*) a bare, two-unit cell Ge/Si multilayer substrate, (*b*) cytochrome *c* covalently tethered to the surface of an 11-siloxyundecanethiol SAM chemisorbed on the substrate for *a* above. The inserts show the diffraction data at higher q_z on an expanded scale. The abscissa is the reciprocal space coordinate, q_z (Å^{-1}), and the ordinate is the natural log of counts collected. The vertical offset in *a* is 8 units.

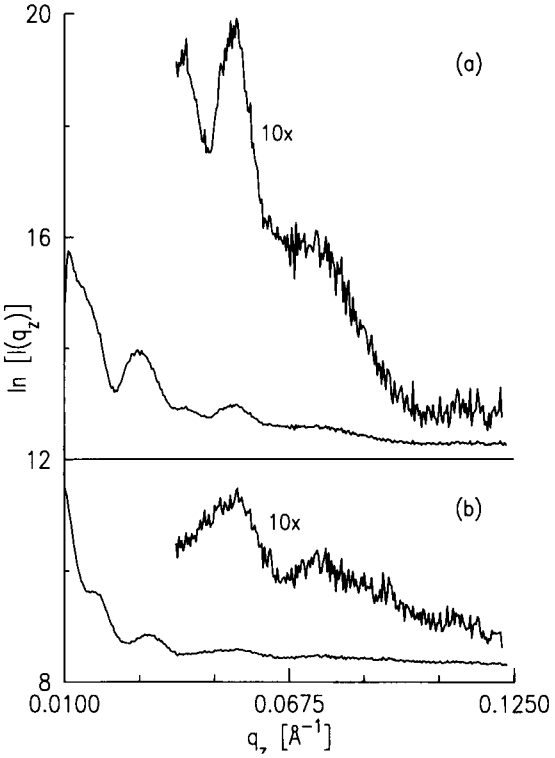

FIGURE 4 Meridional x-ray scattering data, $\ln[I(q_z)]$, for (*a*) a bare, two-unit cell Ge/Si multilayer substrate, (*b*) photosynthetic reaction centers electrostatically tethered to the face of an 11-siloxyundecaneamine SAM chemisorbed on the substrate for *a* above. The inserts show the diffraction data at higher q_z on an expanded scale. The abscissa is the reciprocal space coordinate, q_z (Å^{-1}), and the ordinate is the natural log of counts collected. The vertical offset in *a* is 4 units.

The absolute electron density profile, $\rho_{abs}(z)$, for these multilayer specimens can be expressed mathematically as the sum of the mean electron density profile, $\bar{\rho}(z)$, and the fluctuations about this mean, the electron density contrast profile, $\Delta\rho(z)$ (see Discussion). This mean electron density profile then gives rise to the specular x-ray scattering from the specimen's surface treated in the dynamical diffraction limit, especially for $q_z \leq (q_z)_{crit}$, whereas the electron density contrast profile then gives rise to the kinematical meridional x-ray diffraction over all q_z, as discussed previously (Xu et al.,

1993; Murphy et al., 1993; Blasie et al., 1992). The total meridional elastic x-ray scattering $I(q_z)$, resulting from the specimen's absolute electron density profile, is given in Eq.1.

$$I(q_z) = |F_{tot}(q_z)|^2 = |F_{spec}(q_z)|^2 + |F_{kin}(q_z)|^2 + 2F_{spec}(q_z)F_{kin})(q_z) \quad (1)$$

For $q_z > (q_z)_{crit}$, the specular x-ray scattering $|F_{spec}(q_z)|^2$ approaches 0 rapidly and monotonically and, thus, $|F_{tot}[q_z > (q_z)_{crit}]|^2 \rightarrow |F_{kin}(q_z)|^2$. Therefore, the total meridional x-ray scattering from these multilayer specimens $I(q_z)$ for $(q_z)_{crit} < (q_z)_{min} \leq (q_z) \leq (q_z)_{max}$ is dominated by the kinematical x-ray diffraction arising from the electron density contrast profile, $\Delta\rho(z)$.

The electron density contrast profile of the Ge/Si multilayer substrate contains very narrow, large amplitude features, and its profile structure is essentially known from its MBE fabrication specifications (a comparison of the actual profile structures for the MBE substrates, determined by model refinement analysis of their kinematical meridional x-ray diffraction, with that expected based on their fabrication specifications, is presented in Xu et al., 1993). The SAM/protein overlayers make a relatively small contribution to the profile structure of the composite inorganic multilayer-organic overlayer system, because their electron density contrast profiles are expected to contain broader, smaller amplitude features compared with those of the Ge/Si multilayer. This "known" multilayer substrate profile structure can then be used as the reference structure to determine the profile structures of the unknown SAM/protein overlayers by *x-ray interferometry* (Lesslauer and Blasie, 1971), as indicated below. The kinematical meridional x-ray diffraction for the composite structures, as shown in Figs. 3 *b* and 4 *b*, can be expressed by Eq. 2:

$$|F_{kin}(q_z)|^2 = |F_k(q_z)|^2 + |F_u(q_z)|^2 + 2|F_k(q_z)||F_u(q_z)| \times \cos\{[\Psi_k(q_z) - \Psi_u(q_z)] + [2\pi q_z A_{ku}]\}. \quad (2)$$

where $|F_{kin}(q_z)|^2$ is the total kinematical structure factor modulus squared of the composite structure and $|F_k(q_z)|^2$ and $|F_u(q_z)|^2$ are the kinematical structure factor moduli squared of the known multilayer substrate and the unknown SAM/protein overlayer, respectively. These three structure factor moduli can be obtained experimentally from the kinematical x-ray scattering from the Ge/Si multilayer substrate itself, from the SAM/protein overlayer on a uniform Si substrate, and from the composite structure. Ψ_k and Ψ_u are the phases of their respective structure factors, where Ψ_k is known (because the reference profile structure of the multilayer substrate and, hence, its structure factor, is known) and Ψ_u is unknown. Each are referenced to the center of mass of their respective profile structure, and A_{ku} is the distance along the *z* axis between the centers of mass of the multilayer substrate and the SAM/protein overlayer. If, instead, we reference the center of mass of the profile of the unknown overlayer structure to the center of mass of the profile of the known multilayer reference structure via the substitution $\Psi'_u = [\Psi_u - A_{ku}]$, application of Eq. 2 can provide the unknown Ψ'_u as a function of q_z; a unique inverse Fourier transform utilizing the experimental modulus, $|F_u(q_z)|$, and the thereby determined Ψ'_u then provides the desired unknown profile structure of the SAM/protein overlayer. The effect of the last term in Eq. 2, which corresponds to the critical interference between the strong kinematical diffraction from the multilayer substrate and the weak kinematical scattering from the overlayer *required to recover the otherwise unknown phase information*, Ψ'_u, is readily apparent from the differences between the kinematical diffraction from the bare MBE substrates (Figs. 3 *a* and 4 *a*) and that for the composite multilayer substrate-SAM/protein overlayer specimens (Figs. 3 *b* and 4 *b*). For example, the presence of minima in Figs. 3 *b* and 4 *b* which do not exist in Figs. 3 *a* and 4 *a*, respectively, are indicative of the destructive interference effects.

For $q_z \geq 0.0135$ Å^{-1}, the $|F_{kin}(q_z)|^2$ for both the bare Ge/Si multilayer substrates and the composite inorganic multilayer/organic overlayer specimens were assumed to be obtainable from their Lorentz-corrected meridional x-ray scattering, $I_c(q_z)$, by subtraction of $|F_{spec}(q_z)|^2$, as approximated by the Lorentz-corrected meridional scattering from a uniform silicon substrate (Xu et al., 1993; Murphy et al., 1993). A Lorentz factor of q_z was applied to correct for the ω-oscillation of the specimens (Skita et al., 1986). This procedure resulted in the kinematical diffraction data being restricted to the q_z range $(q_z)_{min} \approx 0.011$ Å$^{-1} \leq q_z \leq (q_z)_{max} \approx 0.115$ Å^{-1}. All Fourier analyses, both via interferometry and holography, were thereby restricted to this q_z window.

X-ray interferometric analysis was implemented using a highly constrained real-space refinement algorithm (Xu et al., 1991) to perform the interferometric phasing of the $|F_{kin}(q_z)|^2$ of the composite system, rather than the point-by-point phasing in q_z space, as described previously (Lesslauer and Blasie, 1971) and briefly above. This alternate approach to the interferometric phasing is particularly important because it can readily allow for (see below) some modification of the surface of the reference multilayer substrate profile structure upon chemisorption of the SAM onto its surface. The relative electron density profile for the "known" Ge/Si multilayer substrate is first established, with the initial models for the two unit cell Ge/Si multilayer substrates being developed on an absolute electron density scale based on the fabrication specifications (see Materials and Methods). Details of the real-space model refinement procedure to obtain the actual profile structure for the multilayer substrate have been described previously (Xu et al., 1993; Murphy et al., 1993). Again, only the *interior* ($Ge_2Si_{30}Ge_2$) portion of this "known" relative electron density profile structure was used as the reference structure for the constrained real-space refinement because of the modification of the outer silicon layer of the substrate upon formation of the SAM on its surface via chemisorption (Xu et al., 1993). Fig.5, *b* and *f* contain the experimental relative electron density profile structures, $\Delta\rho_{exp}(z)$, for the composite Ge/Si

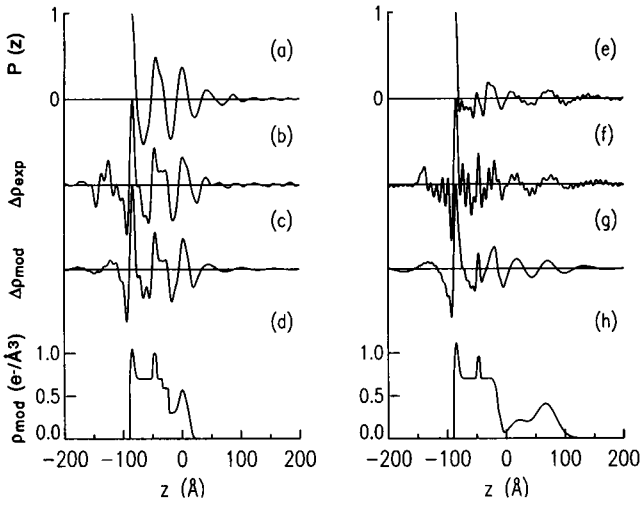

FIGURE 5 (*a*, *e*) Experimental Patterson functions, $P(z)$, uniquely derived from the x-ray diffraction data without phase information, (*b*, *f*) experimental relative electron density profiles, $\Delta\rho_{exp}(z)$, derived via x-ray interferometry, (*c*, *g*) refined model relative electron density profiles, $\Delta\rho_{mod}(z)$, calculated uniquely from *d* and *h*, and (*d*, *h*) refined model absolute electron density profiles, $\rho_{mod}(z)$, for the thiol SAM/cyt *c* and amine SAM/RC specimens, respectively, in units of $e^-/Å^3$. The *z* axis origin is completely arbitrary and determined solely by the positioning of the reference profile structure of the Ge/Si multilayer substrate on the *z* axis.

multilayer-thiol SAM/cyt *c* and -amine SAM/RC specimens, respectively, derived by applying the highly constrained, real-space refinement to their meridional x-ray diffraction data employing the reference structure as a primary constraint.

After the formation of the SAM and protein layers on the surface of these multilayer substrates, additional, more complex features appear at and beyond the profile position of the SiO_x surface of the substrates for $-22\ Å \leq z \leq 15\ Å$ and $-14\ Å \leq z \leq 100\ Å$ for the thiol SAM/cyt *c* and amine SAM/RC systems, respectively. To understand the nature of these new features in the SAM/protein region of the experimental relative electron density profiles, it is necessary to establish real-space, absolute electron density profile models that account for each feature in Fig. 5, *b* and *f*. Fig. 5, *d* and *h* are the refined absolute electron density profiles for the thiol SAM/cyt *c* and the amine SAM/RC systems, respectively. Their corresponding relative electron density profile models are shown in Fig. 5, *c* and *g*, respectively. These relative electron density profile models were produced via a "double" Fourier transform (i.e., {Fourier transform}{inverse Fourier transform}) of the absolute electron density profile models, subject to the same q_z window as the corresponding experimental diffraction data (Xu et al., 1993; Murphy et al., 1993). Subsequent refinement of the model profiles was performed until their relative electron density profiles were essentially identical to the corresponding experimental relative electron density profiles (compare in Fig.5, *b* with *c* and *f* with *g*). A one-to-one correspondence was ultimately found to exist between each feature in the refined relative electron density profile model and its counterpart in the experimental relative electron density profile model, which thereby established both the position (± 0.1 Å) and density level ($\pm 0.01\ e^-/Å^3$) of each feature in the absolute electron density profile model via this real-space refinement. The basis for these precisions has been described elsewhere (Murphy et al., 1993). The two peak features at $z \sim -85$ Å and $z \sim -47$ Å in the relative electron density profile structures were thereby established to arise from the two Ge_2 layers in the two substrates in Fig. 5, *c* and *g*. In the thiol SAM/cyt *c* system, the two interfaces, Si/SiO_x and SiO_x/SAM, are clearly discernible at positions $z \sim -34$ Å and -24 Å, respectively, in Fig. 5 *d*, giving rise to the two smaller peak features $-36\ Å \leq z \leq -23$ Å in Fig. 5 *c*. These two interfaces in the amine SAM/RC system are much broader and are contained over a much smaller region of *z*, namely, $-25\ Å \leq z \leq -3$ Å in Fig. 5 *g–h* (see Discussion). The broad surface peak at $z \sim 1$ Å in Fig. 5 *b*, which was not present in the experimental relative electron density profile for the Ge/Si multilayer substrate/thiol SAM (not shown), indicates that the cytochrome *c* molecular profile is centered 12.5 Å from the surface of the thiol SAM, having a profile width of ~20 Å (FWHM). In Fig. 5 *f*, the reaction center molecular profile gives rise to the two broad peaks at $z \sim 18$ Å and 71 Å, which were not present in the experimental relative electron density profile for the Ge/Si multilayer substrate/amine SAM (not shown). The amine SAM is more disordered than the thiol SAM and, its profile width is somewhat more difficult to determine (see Discussion). Nevertheless, these refined absolute electron density profile models yield rather precise knowledge of the profile structures of the composite Ge/Si multilayer-SAM/protein overlayer systems (see Discussion).

The highly constrained real-space refinement algorithm yields one solution of a finite number of possible solutions for the phase of the kinematical structure factor, where the phase dominance of the known reference structure forces the box-refinement algorithm employed to converge to the local structure most similar to the reference structure (Stroud and Agard, 1979; Makowski, 1981). *X-ray holography* (Lesslauer and Blasie, 1971; Smith, 1969), by analogy to simple off-axis Fourier holography with much longer wavelength radiation, has been used (Xu et al., 1993; Murphy et al., 1993) to prove the correctness of the experimental relative electron density profiles for such composite systems so-derived via x-ray interferometry. *If* the Ge layers within the reference profile structure of the Ge/Si multilayer substrate are sufficiently narrow (as possible with MBE fabrication) *and* A_{ku} is sufficiently large, *then* the unknown profile structure for the organic overlayer itself is reconstructed with minimal distortion at the edge of the Patterson function, $P(z)$, which is uniquely obtained from the kinematical diffraction data via Fourier transformation without utilizing *any* phase information. Fig. 5, *a* and *e* are the Patterson functions for $z \geq 0$ for the thiol SAM/cyt *c* and amine SAM/RC systems, respectively, which have been aligned with their corresponding relative electron density profile structures, Fig. 5 *b* and *f*, such that the origin of the Patterson function is located at the same *z* axis position as the first Ge_2 peak feature in the

corresponding relative electron density profile. Comparison of the features in the Patterson functions and in the corresponding experimental relative electron density profiles over the region -22 Å $\leq z \leq 15$ Å and -14 Å $\leq z \leq 100$ Å for the thiol SAM/cyt *c* and amine SAM/RC systems, respectively, reveals that the Ge_2 peak feature at the left edge of the relative electron density profile is convoluted with the SAM/protein overlayer features at the right edge of the profile in the above regions to reconstruct the latter's features in the Patterson function over the same region. The nearly identical agreement between the SAM/protein overlayer profile features at the edge of the Patterson function and those at the edge of the relative electron density profile indicates that the organic overlayer profile structures derived via x-ray interferometry are, therefore, proven correct by x-ray holography.

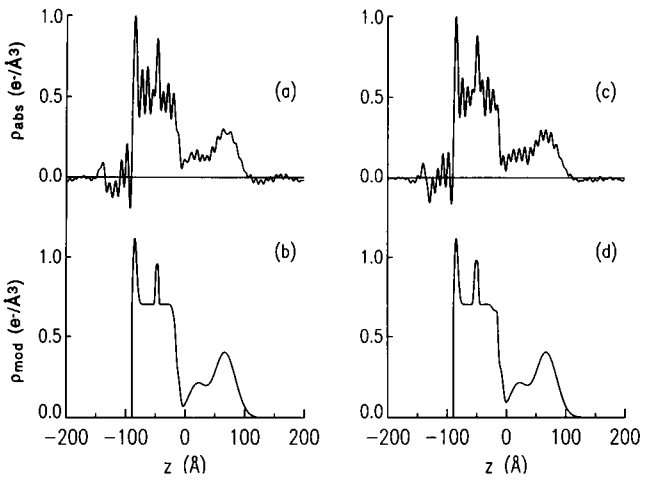

FIGURE 6 (*a*, *c*) Experimental absolute electron density profiles, produced by summation of the mean electron density profiles, $\bar{\rho}_{mod}(z)$, and the experimental relative electron density profiles, $\Delta\rho_{exp}(z)$, to thereby contain only the $(q_z)_{max}$ truncation ripple from the experimental diffraction data, and (*b*, *d*) the refined model absolute electron density profiles, $\rho_{mod}(z)$, for two different amine SAM/RC specimens. The units of the ordinates are $e^-/Å^3$.

DISCUSSION

The SAM/protein overlayer specimens formed on glass substrates used for the optical absorption measurements were prepared *identically and simultaneously* with those on the Ge/Si multilayer substrates used for the x-ray diffraction experiments to ensure that the protein binding measurements could be directly compared with the derived profile structures. The protein binding measurements demonstrated that the binding was highly reproducible and reversible for both SAM/protein systems, employing reduction of the disulfide linkage for the thiol SAM/cyt *c* and high ionic strength buffer for the amine SAM/RC, respectively, to dissociate the protein from its SAM. In addition, they suggested that the tethered protein in each case occurred as a single monolayer on the surface of its SAM.

The profile width of the cytochrome *c* feature and reaction center features within their respective multilayer substrate-SAM/protein profile structures confirm such single monolayer coverage. The covalently tethered cytochrome *c* was found to have a profile width of ~20 Å (FWHM), as was found previously (Pachence and Blasie, 1991). This value corresponds to that for the minor axis of the approximately ellipsoidal cytochrome *c* molecule (see Fig. 9). The reaction center profile width of ~70 Å (FWHM) corresponds to a single monolayer in which the long-axis of the approximately cylindrical reaction center molecule (Pachence et al., 1981; Deisenhofer et al., 1985) is oriented perpendicular to the monolayer plane (see Figs. 7 and 10). This orientation would be expected for detergent-solubilized reaction centers interacting electrostatically with the SAM's surface, as based on prior determinations of the reaction center's molecular structure (Pachence et al., 1979, 1981; Deisenhofer et al., 1985).

The effects of the $(q_z)_{min}$ truncation can be eliminated from the experimental relative electron density profiles, $\Delta\rho_{exp}(z)$, by adding the (very low resolution) mean electron density profile, $\bar{\rho}(z)$, for the refined absolute electron density profile model, whereby only the $(q_z)_{max}$ truncation effects remain. Fig. 6, *a* and *c* show the resulting absolute electron density profiles for *two different* amine SAM/RC specimens. Their corresponding refined absolute electron density models are shown in Fig. 6, *b* and *d*, respectively. The highest spatial frequency components present in the profiles in Fig. 6, *a* and *c* are caused solely by the $(q_z)_{max}$ truncation. The substrate portion of the profiles in Fig. 6, *a* and *b* ($z < -1$ Å) differs slightly from that in Fig. 6, *c* and *d* for the two specimens; however, the amine SAM/RC region ($z > -1$ Å) is virtually identical (Fig. 6, *a* and *c*), aside from the amplitude of the $(q_z)_{max}$ truncation ripple. Given the almost total absence of low spatial frequency $(q_z)_{min}$ oscillations, together with the small amplitude of the $(q_z)_{max}$ truncation ripple in these absolute electron density profiles for $z > 100$ Å, we can estimate that no more than 2–3% of the substrate surface could possess an additional monolayer (or monolayers) of protein.

The absolute electron density profile for the amine SAM/RC system from Fig. 6 *a* is reproduced in Fig. 7 *a* for comparison with previously determined profile structures for photosynthetic reaction centers. First, we considered the profile structure for the reaction center from *Rhodopseudomonas viridis*, which was calculated mathematically from the published crystal structure (Deisenhofer et al., 1985) by subtracting the cytochrome subunit and projecting the three-dimensional structure at atomic resolution onto the long axis of the molecule, as shown in Fig. 7 *b*. This profile structure for this truncated reaction center is asymmetric, possessing two peaks of similar amplitudes, but unequal widths, which differs from the derived profile in Fig. 7 *a* particularly at the cytochrome *c*/amine SAM binding end. This calculated reaction center profile was convoluted with an appropriate Gaussian function to account for the $(q_z)_{max}$-limited spatial resolution of Fig. 7 *a* (Fig. 7 *c*); the so-smoothed profile was found to be slightly asymmetric in the amplitudes of the two peaks, but not to the extent shown in the amine SAM/RC system, in which the first peak nearest the amine-terminated SAM surface has an amplitude approximately half that of the second. This remaining difference might be attributed to the

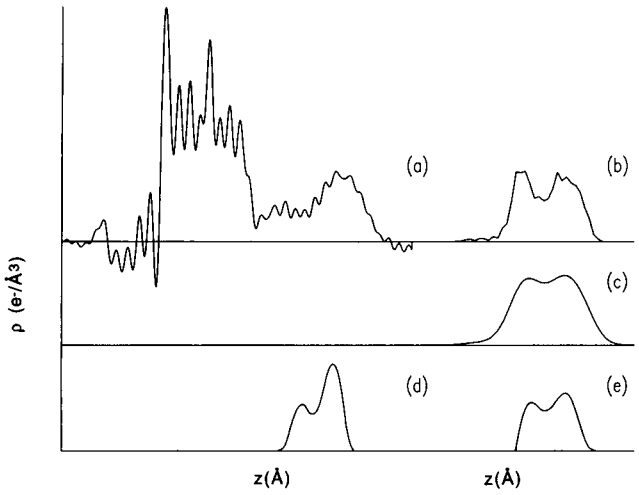

FIGURE 7 (*a*) Experimental absolute electron density profile for an amine SAM/RC specimen (see Fig. 6 *a* for units), (*b*) profile structure calculated from the x-ray crystal structure for the *Rhodopseudomonas viridis* reaction center after truncation of the cytochrome subunit, (*c*) the profile calculated in *b* convoluted with an appropriate Gaussian function to account for the $(q_z)_{max}$ limited spatial resolution, (*d*) previously determined profile structure for the *Rhodopseudomonas sphaeroides* reaction center reconstituted into phospholipid bilayers, and (*e*) previously determined profile structure for the *sphaeroides* reaction center shown in *d* upon binding of cytochrome *c*.

artificial truncation of the cytochrome subunit of the *viridis* reaction center (see below) and/or molecular crowding in the crystal structure. Second, we considered the profile structure for the reaction center used in this study (*Rhodopseudomonas sphaeroides*), determined previously to 9 Å resolution via x-ray and neutron diffraction (Pachence et al., 1981); the reaction centers in this case were reconstituted into phosphatidylcholine bilayers to form oriented multilayers in which the reaction centers were found to be fully functional with near unidirectional vectorial orientation. As can be seen from a comparison of Fig. 7, *a* and *d*, the reaction center profiles for the amine SAM/RC system and the reaction center protein incorporated into lipid bilayers are very similar in their degree of asymmetry at comparable spatial resolution, although their profile widths differ substantially. The latter difference can be accounted for by some axial compression of the reaction center, a demonstrated phenomenon occurring within partially dehydrated oriented multilayers of reconstituted lipid/protein membrane systems (Herbette et al., 1981). It should be noted here that the degree of asymmetry in the profile structure for the *sphaeroides* reaction center taken for Pachence et al. (1981) was later shown in Pachence et al. (1983) to be dependent upon the binding of cytochrome *c* to the reaction center (e.g., at 1:1 mole ratio) *and* that in the presence of one cytochrome *c* bound per reaction center, the asymmetry of the *sphaeroides* reaction center profile structure (Fig. 7 *e*) is virtually identical to that shown in Fig. 7 *c* for the *viridis* reaction center with the cytochrome subunit truncated and subsequently smoothed.

The spatial resolution of the amine SAM/RC electron density profiles permitted the degree of vectorial orientation of the reaction center protein molecules within the tethered monolayer to be assessed. The most relevant reaction center profile determined previously (i.e., the *sphaeroides* profile from Pachence et al. (1981) as discussed above) was used as a model for the reaction center molecular profile in this analysis. Fig. 8 *a* contains the experimental absolute electron density profile, $\rho_{exp}(z) = \{\bar{\rho}(z) + \Delta\rho_{exp}(z)\}$, which contains the $(q_z)_{max}$ truncation effects, and the model absolute electron density profile, $\rho_{mod}(z)$, for the ratios, 100:0 (*dotted line*), 90:10, and 80:20, of the two opposite vectorial orientations of the reaction center protein within the profile for the amine SAM/RC system. Comparison of each $\rho_{mod}(z)$ with the experimental electron density profile, $\rho_{exp}(z)$, in the region of the 0 Å $< z <$ 100 Å clearly demonstrates that the degree of vectorial orientation of the reaction center protein in the profile is essentially 100:0. Only in this limit of a fully unidirectionally oriented reaction center monolayer do the amplitudes of the model electron density profile over this region reach the mean of the $(q_z)_{max}$ truncation ripple in the experimental profile. As the ratios systematically digress from the unidirectional 100:0 extreme, the amplitudes of the two broad peaks at $z \sim$ 18 Å and 70 Å, corresponding to the reaction center protein profile, become increasingly dissimilar to the experimental profile. Because these model profiles were constructed to consist of only the reaction center protein and the inorganic multilayer substrate, the model profiles are slightly less dense in the region of the amine SAM, namely -5 Å $< z <$ 10 Å. Fig. 8 *b* contains the model electron density profiles for the systematically varying ratios, 100:0 (*dotted line*) down to 0:100, i.e., spanning the two extremes of the possible vectorial orientations of the reaction center molecules in the tethered monolayer. The asymmetry of the reaction center profile decreases steadily as the ratios move from the 100:0 extreme orientation, until the peaks are of similar amplitudes for the ratio 50:50, and then reverse and steadily increase the asymmetry as they approach the opposite orientation of 0:100, as anticipated.

It is interesting to compare the results of the thiol SAM/cyt *c* system, in which the yeast cytochrome *c* monolayer is covalently tethered to the thiol-terminated SAM chemisorbed on an inorganic substrate, to previous work (Pachence and Blasie, 1991), where the yeast cytochrome *c* monolayer was covalently tethered to a Langmuir-Blodgett (LB) monolayer of thioethyl stearate (TES) physisorbed on an inorganic substrate, at a comparable spatial resolution. Previously, the ester group of the TES monolayer was found to be distinguishable from the cytochrome *c* in the profile structure. In addition, the FWHM of the cytochrome *c* profile was determined to be consistent with the vectorial orientation derived from the optical linear dichroism (Pachence et al., 1990) and the resonance x-ray diffraction (Pachence et al., 1989) results, in which the heme plane was found to lie, on average, nearly parallel to the surface plane of the LB multilayer yielding a profile width (FWHM) of 20–25 Å. Fig. 9 *a* shows the experimental absolute electron density profile, containing only the $(q_z)_{max}$ truncation ripple, for the thiol SAM/cyt *c* system. The cytochrome *c* region of this

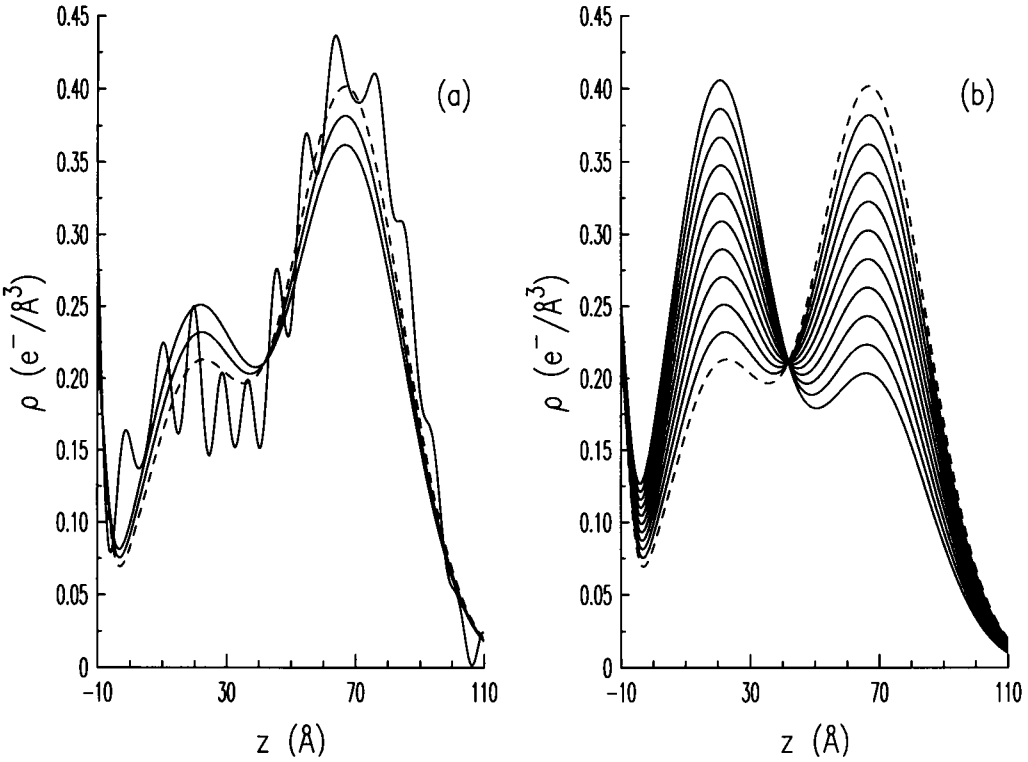

FIGURE 8 (*a*) The experimental absolute electron density profile, $\{\tilde{\rho}(z) + \Delta\rho_{exp}(z)\}$, reproduced from Fig. 6, containing only the $(q_z)_{max}$ truncation ripple, and the refined absolute electron density model profiles for the following ratios of the two opposite vectorial orientations of the reaction center molecular profile within the amine SAM/RC system: 100:0 (*dotted line*), 90:10, and 80:20. (*b*) The refined electron density model profiles, $\rho_{mod}(z)$, for the following ratios of the two opposite vectorial orientations of the reaction center molecular profile within the amine SAM/RC system: 100:0 (*dotted line*), 90:10, 80:20, 70:30, 60:40, 50:50, 40:60, 30:70, 20:80, 10:90, and 0:100. The ordinates have units of $e^-/Å^3$.

profile (*solid line*) is shown in Fig. 9 *b*, as well as the two projections of the x-ray crystal structure at atomic resolution for yeast cytochrome *c* (Louie et al., 1988), containing one surface thiol group at Cys-102 that forms the disulfide linkage with the sulfhydryl-terminated SAM, for both the parallel (*dotted-dashed*) and perpendicular (*dashed*) orientations of the heme plane relative to the substrate plane (the heme group profiles are also shown within the protein profiles). The profile FWHM for the parallel orientation is approximately 20 Å, which agrees well with the experimental profile width and that for the previous studies, whereas the profile FWHM for the perpendicular orientation certainly does not. The cytochrome *c* profile is slightly, but significantly, asymmetric mostly because of the added electron density of the disulfide linkage near the thiol endgroup surface of the SAM, as indicated from the projections of the x-ray crystal structure.

The meridional x-ray diffraction data collected from the SAM/protein systems chemisorbed onto these particular Ge/Si multilayer substrates fabricated by MBE enabled experimental electron density profiles, derived from the data via x-ray interferometry, to be proven correct via x-ray holography. In addition, the MBE substrates were also responsible for the substantially improved spatial resolution in the derived experimental profiles, namely ~7 Å, over that in the previous studies of such tethered protein monolayers using sputtered substrates, namely, >20 Å (Amador et al., 1993). This improved spatial resolution made possible the determination of the degree of vectorial orientation of the protein molecules within the tethered monolayers. Furthermore, the chemically bonded nature of the inorganic multilayer substrate-SAM system, including the protein-specific SAM surface endgroups, has resulted in the ability to orient vectorially both detergent-solubilized integral membrane proteins as well as soluble proteins on the SAM's surface. The specificity of the strong interaction between the SAM surface endgroups with the exposed surface residues of the integral membrane proteins should further enable the replacement of the solubilizing detergent with phospholipid, as in typical membrane reconstitution (Pachence et al., 1979).

Finally, the profile structure of the thiol SAM/cyt *c* system seems to be more ordered than the amine SAM/RC system. This may be because of the smaller protecting group used for the thiol SAM (acetate versus *tert*-butoxycarbonyl) and/or the thiol SAM's smaller substrate-reacting group (trichlorosilane versus triethoxysilane), which could result in the formation of a more densely packed SAM on the surface of the substrate, thereby reducing disordering at the SAM surface upon subsequent deprotection and protein binding. As can be seen from the derived electron density profiles (Fig. 5, *d* and *h*), the profile structures for the thiol SAM/cyt *c* system contain a better defined SAM/protein overlayer as

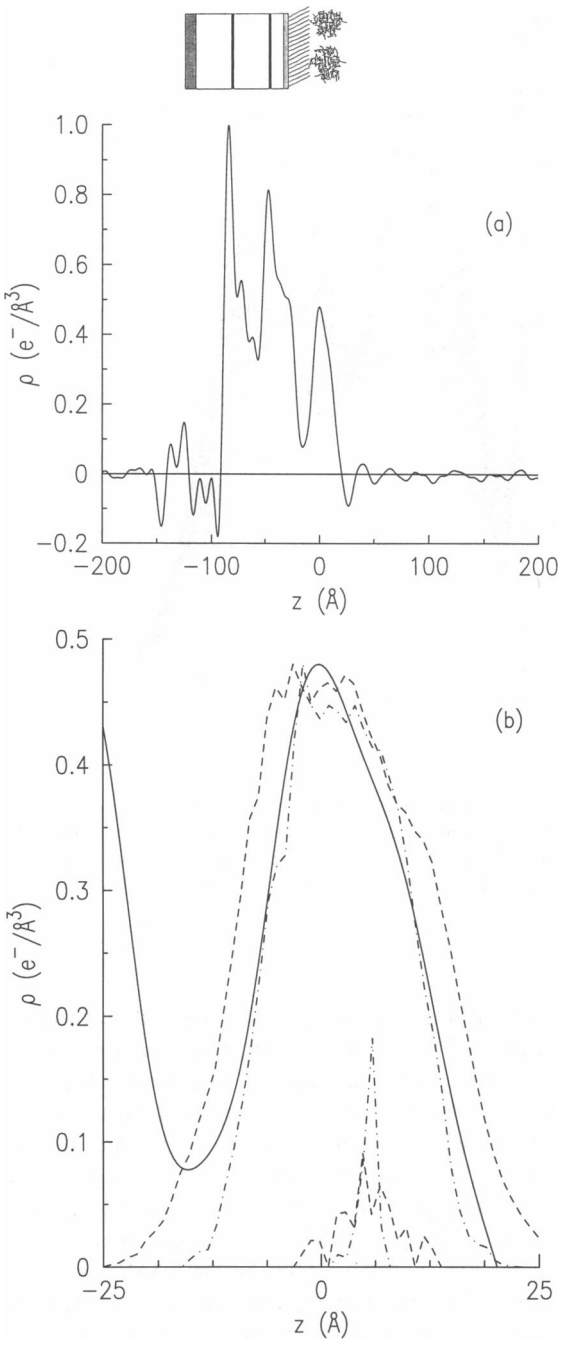

FIGURE 9 (*a*) The absolute experimental electron density profile, produced by summation of the mean electron density profile, $\bar{\rho}_{mod}(z)$, and the experimental relative electron density profile, $\Delta\rho_{exp}(z)$, containing only the $(q_z)_{max}$ truncation ripple from the experimental diffraction data for the thiol SAM/cyt *c* system with the corresponding schematic represented to scale directly above the profile for reference, and (*b*) the profile structure calculated from the x-ray crystal structure of yeast cytochrome *c*, including the addition of the SAM's thiol group to Cys-102, for the parallel (*dotted-dashed*) and perpendicular (*dashed*) orientations of the heme plane relative to the substrate plane. In addition, the corresponding profiles for the heme group are shown. The units for both ordinates are $e^-/Å^3$.

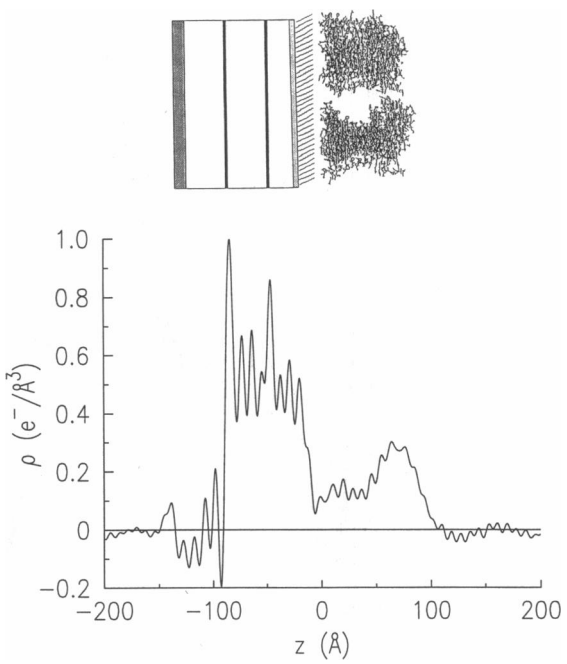

FIGURE 10 The absolute experimental electron density profile (reproduced from Fig. 6 *a* in units of $e^-/Å^3$), produced by summation of the mean electron density profile, $\bar{\rho}_{mod}(z)$, and the experimental relative electron density profile, $\Delta\rho_{exp}(z)$, containing only the $(q_z)_{max}$ truncation ripple from the experimental diffraction data for the amine SAM/RC system with the corresponding schematic represented to scale directly above the profile for reference.

compared with the amine SAM/RC system; the cytochrome *c* profile structure was readily modeled using relatively narrowly defined error functions to describe its electron density profile, as opposed to the broader "wings" of the Gaussian functions used to model the reaction center profile. Studies utilizing pyridyl-terminated SAMs to form subsequently a tethered $(pyridyl)_n$-OsO_4-C_{60} complex on these Ge/Si multilayer substrates support the above conclusion in that they resulted in a sufficiently ordered profile structure in which the $(pyridyl)_n$-OsO_4 and the "fullerene" C_{60} components were distinct (Chupa et al., 1993). This high resolution nature of the profile structure for the organic overlayer seems, in this case, to be caused by the method of SAM formation. The pyridyl-terminated alkylsiloxane monolayers were produced by initially forming bromine-terminated SAMs on the silicon oxide surface of the substrate and subsequently chemically converting these to pyridyl-terminated SAMs. This process results in densely packed, well ordered SAMs because of the relatively small bromine endgroup present during the self-assembly step. Modifications, therefore, are under way to improve the self-assembly method to produce better ordered SAMs by using smaller endgroups on the self-assembly compounds and then performing the necessary chemistry subsequently on the substrate surface. Conversely, it might be important to note that the differences between substrates in the narrowness of the Si/SiO_x and SiO_x/SAM interfaces resulting from the self-assembly process do not seem to be a consequence of the sizes of these endgroups. Nevertheless, the potential spatial resolution in the derived profiles for the SAM/tethered protein systems might in fact be further improved to 3–4 Å resolution by closer attention to the phase

diagram for the MBE fabrication process to produce Ge profile features as narrow as a single atomic monolayer with sharp Ge/Si interfaces (Bean et al., 1984).

CONCLUSIONS

We have demonstrated that organic self-assembled monolayers (SAMs), chemisorbed to inorganic substrates and possessing specific surface endgroups, can be used to bind selectively and reversibly both soluble proteins and detergent-solubilized integral membrane proteins. Both the cytochrome *c* and photosynthetic reaction center molecules, utilized respectively as test cases in this study, formed a *single monolayer* of the protein molecules *possessing a virtually unidirectional vectorial orientation* tethered to the SAM's surface with approximately close-packed in-plane densities. These definitive structural results were obtained utilizing inorganic multilayer substrates, fabricated by molecular beam epitaxy, which enabled us to use x-ray interferometry to derive the profile structures of the composite multilayer substrate-SAM/protein systems to ~7Å resolution and prove their correctness via x-ray holography. Several improvements in the spatial resolution of this work remain possible for the future involving the structural ordering within both the inorganic multilayer substrate and the chemisorbed SAM. Finally, our results demonstrate that these techniques can now be extended to other integral membrane proteins, such as cytochrome oxidase and cytochrome b/c_1, whose three-dimensional atomic resolution structures are not known, to obtain information on their high resolution profile structures, and particularly, the distribution of the metal redox centers within their profile structures, within such SAM/tethered protein systems.

This work was supported primarily by the National Institutes of Health Grant GM33525. In addition, this work was performed while J. A. Chupa was supported by the Biophysical Spectroscopy Training Grant 5T32GM08275-03. Several of the x-ray measurements were performed on the National Biostructures PRT Beamline X9A supported by the National Institutes of Health Research Resource grant RR01633 at the National Synchrotron Light Source, Brookhaven National Laboratory. The reaction centers used in this work were supplied to us by Dr. Chris Moser of Prof. P. Leslie Dutton's group, Department of Biochemistry and Biophysics, University of Pennsylvania.

REFERENCES

Alegria, G., and P. L. Dutton. 1991. Langmuir-Blodgett monolayer films of the *Rhodopseudomonas viridis* reaction center: determination of the order of the hemes in the cytochrome *c* subunit. *Biochim. Biophys. Acta.* 1057: 258–272.

Amador, S. M., J. M. Pachence, R. Fischetti, J. P. McCauley, Jr., A. B. Smith III, and J. K. Blasie. 1993. Use of self-assembled monolayers to covalently tether protein monolayers to the surface of solid substrates. *Langmuir.* 9:812–817.

Balachander, N., and C. N. Sukenik. 1988. Functionalized siloxy-anchored monolayers with exposed amino, azido, bromo, or cyano groups. *Tetrahedron Lett.* 29:5593–5594.

Bean, J. C., L. C. Feldman, A. T. Fiory, S. Nakahara, and I. K. Robinson. 1984. Ge_xSi_{1-x}/Si strained-layer superlattice grown by molecular beam epitaxy. *J. Vac. Sci. Technol.* A2:436–440.

Bean, J. C., and E. A. Sadowski. 1982. Silicon MBE apparatus for uniform high-rate deposition on standard format wafers. *J. Vac. Sci. Technol.* 20:137–142.

Bill, K., R. P. Casey, C. Broger, and A. Azzi. 1980. Affinity chromatography purification of cytochrome *c* oxidase. Use of a yeast cytochrome *c*-thiol-sepharose 4B column. *FEBS Lett.* 120:248–250.

Blasie, J. K., J. M. Pachence, A. Tavormina, P. L. Dutton, J. Stamatoff, P. Eisenberger, and G. Brown. 1983. The location of redox centers in the profile structure of a reconstituted membrane containing a photosynthetic reaction center-cytochrome *c* complex by resonance x-ray diffraction. *Biochim. Biophys. Acta.* 723:350–357.

Blasie, J. K., J. M. Pachence, A. Tavormina, M. Erecinska P. L. Dutton, J. Stamatoff, P. Eisenberger, and G. Brown. 1982. The location of redox centers in biological membranes determined by resonance x-ray diffraction. II. Analysis of the resonance diffraction data. *Biochim. Biophys. Acta.* 679:188–197.

Blasie, J. K., S. Xu, M. Murphy, J. Chupa, J. P. McCauley, Jr., A. B. Smith III, L. J. Peticolas, and J. C. Bean. 1992. Profile structures of macromolecular monolayers on solid substrates by x-ray interferometry/holography. *Mat. Res. Soc. Symp. Proc.* 237:399–409.

Chupa, J. A., S. Xu, R. F. Fischetti, R. M. Strongin, J. P. McCauley, Jr., A. B. Smith III, J. K. Blasie, L. J. Peticolas, and J. C. Bean. 1993. A monolayer of C_{60} tethered to the surface of an inorganic substrate: assembly and structure. *J. Am. Chem. Soc.* 115:4383–4384.

Clayton, R. K., and R. T. Wang. 1971. Photochemical reaction centers from *Rhodopseudomonas sphaeroides. Methods Enzymol.* 23:696–704.

Deisenhofer, J., O. Epp, K. Miki, R. Huber, and H. Michel. 1985. Structure of the protein subunits in the photosynthetic reaction centre of *Rhodopseudomonas viridis* at 3 Å resolution. *Nature (Lond.).* 318: 618–624.

Fischetti, R., M. Filipkowski, A. Garito, and J. K. Blasie. 1988. Profile structures of ultrathin periodic and nonperiodic multilayer films containing a disubstituted diacetylene by high resolution x-ray diffraction. *Phys. Rev. B.* 37:4714–4726.

Gruner, S. M. 1981. Controlled humidity gas circulators. *Rev. Sci. Instrum.* 52:131–134.

Gunner, M. R., D. E. Robertson, and P. L. Dutton. 1986. Kinetic studies on the reaction center protein from *Rhodopseudomonas sphaeroides*: the temperature and free energy dependence of electron transfer between various quinones in the Q_A site and the oxidized bateriochlorophyll dimer. *J. Phys. Chem.* 90:3783–3795.

Herbette, L., A. Scarpa, J. K. Blasie, C. Wang, A. Saito, and S. Fleischer. 1981. Comparison of the profile structures of isolated and reconstituted sarcoplasmic reticulum membranes. *Biophys. J.* 36:47–72.

Lesslauer, W., and J. K. Blasie. 1971. X-ray holographic interferometry in the determination of planar multilayer structures. Theory and experimental observations. *Acta Crystallogr.* A27:456–461.

Louie, G. V., W. L. B. Hutcheon, and G. D. Brayer. 1988. Yeast iso-1-Cytochrome *c*. A 2.8 Å resolution three-dimensional structure determination. *J. Mol. Biol.* 199:295–314.

Lukevics, E., Z. V. Belyakova, M. G. Pomerantseva, and M. G. Voronkov. 1977. Hydrosilylation. Recent achievements. *In* Journal of Organometallic Chemistry Library 5: Organometallic Chemistry Reviews. Chapt. 1. D. Seyferth, A. G. Davies, E. O. Fischer, J. F. Normant, and O. A. Reutov, editors. Elsevier, Amsterdam. 1–179.

Makowski, L. 1981. The use of continuous diffraction data as a phase constraint. I. One-dimensional theory. *J. Appl. Cryst.* 14:160–168.

Murphy, M. A., J. K. Blasie, L. J. Peticolas, and J. C. Bean. 1993. X-ray interferometry/holography for the unambiguous determination of the profile structures of single Langmuir-Blodgett monolayers. *Langmuir.* 9:1134–1141.

Pachence, J. M., S. Amador, G. Maniara, J. Vanderkooi, P. L. Dutton, and J. K. Blasie. 1990. Orientation and lateral mobility of cytochrome *c* on the surface of ultrathin lipid multilayer films. *Biophys. J.* 58:379–389.

Pachence, J. M., and J. K. Blasie. 1987. The location of cytochrome *c* on the surface of ultrathin lipid multilayer films using x-ray diffraction. *Biophys. J.* 52:735–747.

Pachence, J. M., and J. K. Blasie. 1991. Structural investigation of the covalent and electrostatic binding of yeast cytochrome *c* to the surface of various ultrathin lipid multilayers using x-ray diffraction. *Biophys. J.* 59:894–900.

Pachence, J. M., P. L. Dutton, and J. K. Blasie. 1979. Structural studies on reconstituted reaction center-phosphatidylcholine membranes. *Biochim. Biophys. Acta.* 548:348–373.

Pachence, J. M., P. L. Dutton, and J. K. Blasie. 1981. The reaction center profile structure derived from neutron diffraction. *Biochim. Biophys. Acta.* 635:267–283.

Pachence, J. M., P. L. Dutton, and J. K. Blasie. 1983. A structural investigation of cytochrome *c* binding to photosynthetic reaction centers in reconstituted membranes. *Biochim. Biophys. Acta.* 724:6–19.

Pachence, J. M., R. F. Fischetti, and J. K. Blasie. 1989. Location of the heme-Fe atoms within the profile structure of a monolayer of cytochrome *c* bound to the surface of an ultrathin lipid multilayer film. *Biophys. J.* 56:327–337.

Sagiv, J. 1980. Organized monolayers by adsorption. I. Formation and structure of oleophobic mixed monolayers on solid surfaces. *J. Am. Chem. Soc.* 102:92–98.

Skita, V., M. Filipkowski, A. F. Garito, and J. K. Blasie. 1986. Profile structures of very thin multilayers by x-ray diffraction using direct and refinement methods of analysis. *Phys. Rev. B.* 34:5826–5837.

Smith, H. M. 1969. Principles of Holography. Wiley-Interscience, New York. 239 pp.

Stamatoff, J., P. Eisenberger, J. K. Blasie, J. M. Pachence, A. Tavormina, M. Erecinska, P. L. Dutton, and G. Brown. 1982. The location of redox centers in biological membranes determined by resonance x-ray diffraction. I. Observation of the resonance effect. *Biochim. Biophys. Acta.* 679: 177–87.

Steinemann, A., and P. Lauger. 1971. Interaction of cytochrome *c* with phospholipid monolayers and bilayer membranes. *J. Membr. Biol.* 4: 74–86.

Stroud, R. M., and D. A. Agard. 1979. Structure determination of asymmetric membrane profiles using an iterative Fourier method. *Biophys. J.* 25:495–514.

Wasserman, S. R., H. Biebuyck, and G. M. Whitesides. 1989. Monolayers of 11-trichlorosilylundecyl thioacetate: a system that promotes adhesion between silicon dioxide and evaporated gold. *J. Mater. Res.* 4:886–892.

Xu, S., R. F. Fischetti, J. K. Blasie, L. J. Peticolas, and J. C. Bean. 1993. Profile and in-plane structures of self-assembled monolayers on Ge/Si multilayer substrates by high-resolution x-ray diffraction employing x-ray interferometry/holography. *J. Phys. Chem.* 97:1961–1969.

Xu, S., M. A. Murphy, S. M. Amador, and J. K. Blasie. 1991. Proof of the asymmetry in the Cd-arachidate bilayers of ultrathin Langmuir-Blodgett multilayer films via x-ray interferometry. *J. Phys. I France.* 1:1131–1144.